JOURNAL OF SOLID STATE CHEMISTRY 113, 168–175 (1994)

Preparation and Crystal Structure of $Na_2Zn(HPO_4)_2 \cdot 4H_2O$, a New Layered Sodium Zinc Phosphate Containing "Bifurcated" Tetrahedral 12-Rings

William T. A. Harrison,*[1] Tina M. Nenoff,† Thurman E. Gier,‡ and Galen D. Stucky‡

*Department of Chemistry, University of Houston, Houston, Texas 77204-5641; †Sandia National Laboratories, Albuquerque, New Mexico 87145; and ‡Department of Chemistry, University of California, Santa Barbara, California 93106-9510

Received November 29, 1993; in revised form February 9, 1994; accepted February 11, 1994

We report the low-temperature (~0°C) synthesis and X-ray single-crystal structure of $Na_2Zn(HPO_4)_2 \cdot 4H_2O$, a new layered material, whose structure is built up from sheets of vertex-sharing ZnO_4 and HPO_4 tetrahedra, which encapsulate octahedrally coordinated "guest" sodium cations and water molecules. The Zn/P tetrahedral-atom connectivity in $Na_2Zn(HPO_4)_2 \cdot 4H_2O$ results in a two-dimensional network of layers of "bifurcated," tetrahedral 12-rings, with interlayer connectivity established only by sodium cations and via H bonds. X-ray powder data and ^{31}P MAS NMR spectra are consistent with those expected from the crystal structure data. Crystal data are $Na_2Zn(HPO_4)_2 \cdot 4H_2O$ ($ZnNa_2P_2O_{12}H_{10}$), $M_r = 375.37$, monoclinic, space group $P2_1/c$ (No. 14), $a = 8.947(2)$ Å, $b = 13.254(2)$ Å, $c = 10.098(2)$ Å, $\beta = 116.358(6)°$, $V = 1074.5$ Å^3, $Z = 4$, $R = 4.25\%$, and $R_w = 5.68\%$ [1608 unique reflections with $I > 3\sigma(I)$].

INTRODUCTION

Novel, nonaluminosilicate framework materials are currently of considerable interest with respect to the possibility of obtaining extended structures containing very large pores. The mineral cacoxinite (1), a mixed octahedral/tetrahedral-framework aluminum/iron/phosphate, and the recently prepared "cloverite" (2), a synthetic gallofluorophosphate, both contain channels with diameters exceeding 14 Å. A newly characterized vanadophosphate containing organic guest species (3) indicates the importance of hydrothermal methods in synthesizing new, microporous structures.

Our own work has recently focused on preparing new phases containing beryllium or zinc in combination with phosphorus or arsenic as the tetrahedral-framework atoms (here denoted as BePOs, ZnPOs, BeAsOs, and ZnAsOs, respectively). Many new materials have already been reported (4), including several analogues of aluminosilicate (AlSiO) zeolites and novel phases which have no known AlSiO congeners. Zeolite analogues include ZnPO and BePO faujasites (5), BePO and BeAsO zeolite rhos (4), ZnPO, ZnAsO, BePO, and BeAsO sodalites (6, 7), and ZnPO, ZnAsO, BePO, and BeAsO Li–A-type phases (4). Novel BePO (8) and ZnPO (9, 10) phases result when organic cations are used in the synthesis procedure. Other new materials in the Be/Zn/P/As/O phase space consist of one-dimensional tetrahedral chain ions containing 3-ring groupings (11) and the nonisostructural two-dimensional layered phases $MH(ZnPO_4)_2$ (M = Cs, Na), in which the 3-ring-containing Zn/P/O layers sandwich alkali-metal cations (12).

This paper reports the synthesis, crystal structure, and ^{31}P MAS NMR spectra of $Na_2Zn(HPO_4)_2 \cdot 4H_2O$, a new layered, two-dimensional zincophosphate material containing interlinked "bifurcated" tetrahedral 12-rings, which complements our recent systematic study (13) of mild-condition reactions in the Na/Zn/P/O phase space.

SYNTHESIS AND PHYSICAL CHARACTERIZATION

$Na_2Zn(HPO_4)_2 \cdot 4H_2O$ was prepared by a low-temperature method as follows: 8.28 g of $NaH_2PO_4 \cdot H_2O$ (60 mmol), 3.462 g of 4 M NaOH (12 mmol), and 20 ml of H_2O were mixed in a Teflon bottle, resulting in a clear solution, which was then cooled to ~ −15°C in a freezer. To the mixture was added 7.71 g of precooled 2 M $Zn(NO_3)_2$ solution (12 mmol), resulting in a milky solution. The bottle was immediately returned to the freezer and held there for 30 min, and then placed in a freezer at 4°C for 4 days. The resultant pH was 3, and 1.60 g of crystalline material was recovered by vacuum filtration and air drying. Crystals of $Na_2Zn(HPO_4)_2 \cdot 4H_2O$ appear to be indefinitely stable in air.

X-ray powder data [Scintag automated PAD-X diffractometer, θ–θ geometry, flat plate sample, CuKα radiation, $\bar{\lambda} = 1.54178$ Å, $T = 25(2)$°C] were collected for a thor-

[1] To whom correspondence should be addressed.

0022-4596/94 $6.00

TABLE 1
X-Ray Powder Data for $Na_2Zn(HPO_4)_2 \cdot 4H_2O$

h	k	l	$2\theta_{obs}$	$\Delta(2\theta)^a$	d_{calc}	$\Delta(d)^b$	$I_{rel}{}^c$
1	0	0	10.963	−0.041	8.033	0.030	58
0	1	1	11.789	−0.026	7.484	0.016	100
1	1	−1	12.831	−0.033	6.876	0.018	50
0	2	0	13.294	−0.014	6.647	0.007	5
0	2	1	16.513	−0.017	5.358	0.006	4
1	2	0	17.284	−0.017	5.121	0.005	12
1	0	−2	17.629	−0.069	5.007	0.020	27
1	1	1	18.904	−0.019	4.686	0.005	19
2	0	0	22.087	−0.024	4.017	0.004	59
0	3	1	22.345	0.027	3.980	−0.005	22
1	3	0	22.891	−0.010	3.880	0.002	10
2	1	0	23.081	−0.031	3.845	0.005	30
2	2	−2	25.867	−0.027	3.438	0.004	23
1	3	1	26.833	−0.012	3.318	0.001	18
1	1	−3	27.308	−0.060	3.256	0.007	15
0	3	2	28.145	−0.010	3.167	0.001	9
2	1	−3	28.751	−0.046	3.098	0.005	22
1	4	−1	29.046	−0.006	3.071	0.001	21
1	2	2	29.763	−0.020	2.997	0.002	11
2	3	−2	29.969	−0.030	2.976	0.003	10
3	0	−2	30.232	−0.059	2.948	0.006	35
3	1	−2	31.029	−0.016	2.878	0.002	35
1	4	1	32.307	0.003	2.769	−0.000	20
0	2	3	32.526	−0.027	2.748	0.002	42
3	2	−2	33.185	−0.030	2.695	0.002	30
0	4	2	33.419	0.000	2.679	−0.000	39
2	4	−2	35.042	0.029	2.561	−0.002	8
2	0	−4	35.836	−0.001	2.504	0.000	6
3	2	−3	36.093	−0.038	2.484	0.003	32
2	1	2	36.516	0.025	2.460	−0.002	29
1	5	1	38.333	0.034	2.348	−0.002	14
1	2	−4	38.639	−0.006	2.328	0.000	7
2	5	−2	40.692	0.032	2.217	−0.002	4
3	2	1	41.448	0.014	2.178	−0.001	12
4	1	−3	42.132	0.079	2.147	−0.004	5
4	2	−1	43.747	−0.003	2.067	0.000	5
1	4	3	45.576	0.042	1.991	−0.002	12
2	6	−2	46.762	−0.024	1.940	0.001	12
5	3	−3	55.513	0.036	1.655	−0.001	5
3	0	−6	55.087	0.119	1.669	−0.003	14
5	3	−1	57.489	0.021	1.602	−0.001	8
4	4	−5	58.225	−0.036	1.582	0.001	12
1	2	5	58.613	−0.016	1.573	0.000	6

[a] $2\theta_{obs} - 2\theta_{calc}$.
[b] $d_{obs} - d_{calc}$.
[c] $100 \times I/I_{max}$.

TABLE 2
Crystallographic Parameters for $Na_2Zn(HPO_4)_2 \cdot 4H_2O$

Empirical formula	$ZnP_2Na_2O_{12}H_{10}$
Formula weight	375.37
Habit	Transparent lump
Crystal size (mm)	0.4 × 0.3 × 0.3
Crystal system	Monoclinic
a(Å)	8.947(2)
b(Å)	13.254(2)
c(Å)	10.098(2)
β(°)	116.358(6)
V(Å^3)	1074.5
Z	4
Space group	$P2_1/c$ (No. 14)
T(°C)	25(2)
λ(Mo$K\alpha$)(Å)	0.71073
ρ_{calc}(g/cm^3)	2.32
μ(Mo$K\alpha$)(cm^{-1})	27.64
Absorption correction	None
hkl data limits	$-10 \le 9, 0 \le 16, 0 \le 12$
Total data	2878 ($2\theta < 53°$)
Observed data[a]	1608
Parameters	180
$R(F)^b$(%)	4.25
$R_w(F)^c$(%)	5.68

[a] $I > 3\sigma(I)$ after merging.
[b] $R = 100 \times \Sigma| |F_o| - |F_c| |/\Sigma|F_o|$.
[c] $R_w = 100 \times [\Sigma w(|F_o| - |F_c|)^2/\Sigma w|F_o|^2]^{1/2}$, with $w_i = 1/\sigma_i^2$.

oughly ground sample of $Na_2Zn(HPO_4)_2 \cdot 4H_2O$. The instrumental $K\alpha_1/K\alpha_2$ profile was reduced to a single Cu$K\alpha_1$ peak (λ = 1.540568 Å) by a software "stripping" routine, and d-spacings were established using silicon powder (a = 5.43035 Å) as an internal standard, relative to this wavelength. The powder pattern was indexed using the $Na_2Zn(HPO_4)_2 \cdot 4H_2O$ single-crystal cell parameters, and the lattice parameters were optimized by least-squares refinements using Scintag software routines, resulting in refined values of a = 8.964(4) Å, b = 13.294(7) Å, c = 10.104(4) Å, and β = 116.34(3)°(V = 1079.0 Å^3). The powder pattern of $Na_2Zn(HPO_4)_2 \cdot 4H_2O$ is listed in Table 1.

^{31}P and $^{31}P\{^1H\}$ MAS NMR spectra of $Na_2Zn(HPO_4)_2 \cdot 4H_2O$ were collected on a General Electric GN-300 spectrometer (121.65 MHz; field strength, 7.05 T), with 80 and 31 acquisitions, respectively, using a multinuclear broadband MAS NMR probe from Doty Scientific. Data were collected in single-pulse mode, with a 45° pulse length of 3 μsec and a recycle delay time of 5 min. The spectra were identical: two distinct, overlapping shifts at 5.67 and 4.42 ppm (relative to 85% H_3PO_4).

STRUCTURE DETERMINATION

A suitable crystal of $Na_2Zn(HPO_4)_2 \cdot 4H_2O$ was selected for structure determination and mounted on a thin glass fiber with cyanoacrylate glue. Preliminary X-ray scans indicated instrumental-resolution (ω-scan < 0.2°) peak widths. Room-temperature [25(2)°C] intensity data were collected on a Huber automated four-circle diffractometer (graphite-monochromated Mo$K\alpha$ radiation, λ = 0.71073 Å) as outlined in Table 2. Initially, 27 reflections were located and centered by searching reciprocal space (8° < 2θ < 30°) and indexed to obtain a unit cell and orientation

TABLE 3
Atomic Positional/Thermal Parameters for $Na_2Zn(HPO_4)_2 \cdot 4H_2O$

Atom	x	y	z	$U_{eq}{}^a/U_{iso}{}^b$
Na(1)	0.1632(3)	0.9663(2)	0.3589(3)	0.0271
Na(2)	0.3201(3)	0.7748(2)	0.1988(3)	0.0281
Zn(1)	0.59604(8)	0.84017(5)	0.03728(7)	0.0170
P(1)	0.2564(2)	0.9385(1)	−0.1105(2)	0.0161
P(2)	0.7258(2)	0.6865(1)	0.2950(2)	0.0154
O(1)	0.3702(5)	0.8561(3)	−0.1193(4)	0.0214
O(2)	0.6989(5)	0.9587(3)	0.1509(4)	0.0223
O(3)	0.5777(5)	0.7378(3)	0.1700(4)	0.0190
O(4)	0.7297(5)	0.7883(3)	−0.0562(4)	0.0201
O(5)	0.2561(5)	0.9373(3)	0.0389(4)	0.0255
O(6)	0.0760(5)	0.9164(3)	−0.2373(4)	0.0209
O(7)	0.7020(6)	0.5699(3)	0.2666(5)	0.0233
O(8)	0.8891(5)	0.7180(3)	0.2944(5)	0.0209
O(10)	0.2514(6)	1.0729(3)	0.5582(5)	0.0321
O(11)	0.9417(6)	0.1473(4)	0.8354(5)	0.0364
O(12)	0.8735(5)	0.1603(4)	0.4900(5)	0.0307
O(13)	0.5814(5)	0.1148(3)	0.5890(5)	0.0265
H(61)	0.025(5)	0.861(5)	−0.214(5)	0.09(1)*
H(71)	0.72(1)	0.534(1)	0.353(3)	0.09(1)*
H(101)	0.26(1)	1.144(1)	0.556(9)	0.09(1)*
H(102)	0.27(1)	1.058(6)	0.656(4)	0.09(1)*
H(111)	0.95(1)	0.104(6)	0.913(6)	0.09(1)*
H(112)	1.039(7)	0.188(6)	0.876(8)	0.09(1)*
H(121)	0.961(8)	0.203(6)	0.553(8)	0.09(1)*
H(122)	0.91(1)	0.134(7)	0.422(8)	0.09(1)*
H(131)	0.538(9)	0.147(6)	0.495(6)	0.09(1)*
H(132)	0.490(6)	0.078(6)	0.589(9)	0.09(1)*

[a] $U_{eq}(Å^2) = (U_1U_2U_3)^{1/3}$.

matrix. The initial unit-cell parameters were optimized by least-squares refinement, resulting in monoclinic cell constants of $a = 8.947(2)$ Å, $b = 13.254(2)$ Å, $c = 10.098(2)$ Å, and $\beta = 116.358(6)°$ (digits in parentheses = e.s.d's). Intensity data were collected in the θ–2θ scanning mode for $0 < 2\theta < 53°$ with three standard reflections monitored every 100 observations for intensity variation throughout the course of the experiment: no significant variation in these standards were observed. The scan speed was 6°/min with a scan range of 1.3° below $K\alpha_1$ to 1.6° above $K\alpha_2$. Crystal absorption was monitored by measuring ψ-scans through 360° for selected reflections with $\chi \sim 90°$, but no absorption correction was applied. The raw intensities were reduced to F and $\sigma(F)$ values by using a Lehmann–Larsen profile-fitting routine (14), and the normal corrections for Lorentz and polarization effects were made. Systematic absences in the reduced data ($h0l$, $l \neq 2n$; $0k0$, $k \neq 2n$) unambigously indicated space group $P2_1/c$ (No. 14). A total of 2878 reflection maxima were scanned, of which 1608 were used in the structure solution and refinement [merging $R = 3.9\%$; reflections with $I < 3\sigma(I)$ considered unobserved].

A direct-methods solution for the heavy atom (Zn, P) sites and some of the light atom (Na, O) positions was obtained from the program SHELXS-86 (15), and the remaining atom positions were located from Fourier difference maps following refinement of the known atoms positions. The least-squares, Fourier, and subsidiary calculations were performed using the Oxford CRYSTALS system (16), running on a DEC Micro VAX 3100 computer. Final full-matrix refinements were against F and included anistropic temperature factors for the nonhydrogen atoms and a Larson-type secondary extinction correction (17). Neutral-atom scattering factors, taking account of anomalous dispersion terms, were obtained from "International Tables" (18). Bond-distance/bond-angle restraints [d(O–H) = 0.95(1) Å; θ(H–O–H) = 105(1)°] were used to stabilize the hydrogen-atom positions during the refinement.

Final residuals of $R(F) = 4.25\%$ and $R_w(F) = 5.68\%$ ($w_i = 1/\sigma_i^2$) were obtained. Difference Fourier maps at the end of the refinement revealed no regions of electron density which could be modeled as additional atomic sites (min = −0.7, max = 0.5 electron $Å^{-3}$), and analysis of the various trends in F_o versus F_c revealed no unusual effects. The crystallographic and data-collection parameters are summarized in Table 2; tables of anisotropic ther-

TABLE 4
Bond Distances (Å) for $Na_2Zn(HPO_4)_2 \cdot 4H_2O$

Na(1)–O(6)	2.486(5)	Na(1)–O(7)	2.510(5)
Na(1)–O(10)	2.293(5)	Na(1)–O(11)	2.316(5)
Na(1)–O(12)	2.385(5)	Na(1)–O(13)	2.367(5)
Na(2)–O(1)	2.419(5)	Na(2)–O(3)	2.499(4)
Na(2)–O(5)	2.598(5)	Na(2)–O(11)	2.443(5)
Na(2)–O(12)	2.453(5)	Na(2)–O(13)	2.416(5)
Zn(1)–O(1)	1.952(4)	Zn(1)–O(2)	1.922(4)
Zn(1)–O(3)	1.964(4)	Zn(1)–O(4)	1.949(4)
P(1)–O(1)	1.522(4)	P(1)–O(2)	1.524(4)
P(1)–O(5)	1.510(4)	P(1)–O(6)	1.584(4)
P(2)–O(3)	1.528(4)	P(2)–O(4)	1.524(4)
P(2)–O(7)	1.567(4)	P(2)–O(8)	1.524(4)
O(2)···H(102)	1.86(1)	O(3)···H(131)	1.94(3)
O(4)···H(101)	1.91(1)	O(4)···H(112)	2.09(5)
O(5)···H(71)	1.63(2)	O(5)···H(111)	2.18(7)
O(6)–H(61)	0.95(1)	O(6)···H(122)	2.04(2)
O(7)–H(71)	0.95(1)	O(8)···H(61)	1.64(2)
O(8)···H(121)	1.86(2)	O(10)–H(101)	0.95(1)
O(10)–H(102)	0.95(1)	O(10)···H(132)	2.02(5)
O(11)–H(111)	0.95(1)	O(11)–H(112)	0.95(1)
O(12)–H(121)	0.95(1)	O(12)–H(122)	0.95(1)
O(13)–H(131)	0.96(1)	O(13)–H(132)	0.95(1)

Note. H-bond contacts are indicated by ···.

TABLE 5
Selected Bond Angles (°) for $Na_2Zn(HPO_4)_2 \cdot 4H_2O$

O(2)–Zn(1)–O(1)	116.6(2)	O(3)–Zn(1)–O(1)	105.0(2)
O(3)–Zn(1)–O(2)	108.6(2)	O(4)–Zn(1)–O(1)	106.5(2)
O(4)–Zn(1)–O(2)	110.0(2)	O(4)–Zn(1)–O(3)	110.0(2)
O–Zn(1)–O	109.5[4.1][a]		
O(2)–P(1)–O(1)	111.3(2)	O(5)–P(1)–O(1)	110.3(2)
O(5)–P(1)–O(2)	113.2(2)	O(5)–P(1)–O(1)	106.9(2)
O(6)–P(1)–O(2)	104.1(2)	O(5)–P(1)–O(5)	110.7(2)
O–P(1)–O	109.4[3.3][a]		
O(4)–P(2)–O(3)	110.5(2)	O(7)–P(2)–O(3)	106.7(2)
O(7)–P(2)–O(4)	109.8(2)	O(8)–P(2)–O(3)	111.0(2)
O(8)–P(2)–O(4)	109.9(2)	O(8)–P(2)–O(7)	108.8(2)
O–P(2)–O	109.5[1.6][a]		
P(1)–O(1)–Zn(1)	120.7(2)	P(1)–O(2)–Zn(1)	133.0(3)
P(2)–O(3)–Zn(1)	124.5(2)	P(2)–O(4)–Zn(1)	130.5(2)
P–O–Zn	127.2[5.6][b]		
H(101)···O(4)···H(112)	97.2(33)	H(71)···O(5)···H(111)	86.7(37)
P(1)–O(6)–H(61)	112.1(10)	P(2)–O(7)–H(71)	112.0(10)
H(61)···O(8)···H(121)	96.9(28)	H(101)–O(10)···H(102)	104.9(10)
H(101)–O(10)···H(132)	82.5(62)	H(102)–O(10)–H(132)	99.2(61)
H(111)–O(11)–H(112)	104.9(10)	H(121)–O(12)–H(122)	105.2(10)
H(131)–O(13)–H(132)	105.0(10)		
O(6)–H(61)···O(8)	163.5(42)	O(5)···H(71)–O(7)	158.1(27)
O(4)···H(101)–O(10)	176.2(82)	O(2)···H(102)–O(10)	174.6(69)
O(5)···H(111)–O(11)	124.5(65)	O(4)···H(112)–O(11)	146.1(61)
O(8)···H(121)–O(12)	168.8(72)	O(6)···H(122)–O(12)	165.1(71)
O(3)···H(131)–O(13)	163.9(82)	O(10)···H(132)–O(13)	149.6(76)

Note. H-bond contacts are indicated by ···.
[a] Average bond angle about central atom, with standard deviation in [ ].
[b] Average P–O–Zn angle, with standard deviation in [ ].

mal parameters and observed and calculated structure factors are available as supplementary material from the authors.

RESULTS

Final atomic positional and equivalent thermal parameters for $Na_2Zn(HPO_4)_2 \cdot 4H_2O$ are listed in Table 3, and selected bond distance/angle data are given in Tables 4 and 5, respectively. The asymmetric framework unit and atom labeling scheme are shown in Fig. 1 (program, ORTEP), and the complete crystal structure is illustrated in Figs. 2 and 3.

$Na_2Zn(HPO_4)_2 \cdot 4H_2O$ has a new layer structure, built up from a network of ZnO_4 and HPO_4 tetrahedral subunits. The zinc atom makes four bonds to phosphorus atom neighbors [2 × P(1), 2 × P(2)] via oxygen-atom bridges [one each of O(1) to O(4)], and has typical average geometrical parameters [d_{av}(Zn–O) = 1.947(2) Å]. Both phosphorus atoms make two bonds to neighboring, distinct zinc atoms via O atoms, and their other two oxygen-atom vertices are to a terminal –OH group and an "unsaturated" =O atom, respectively. These three different types of P–O bonds show their expected differentiation

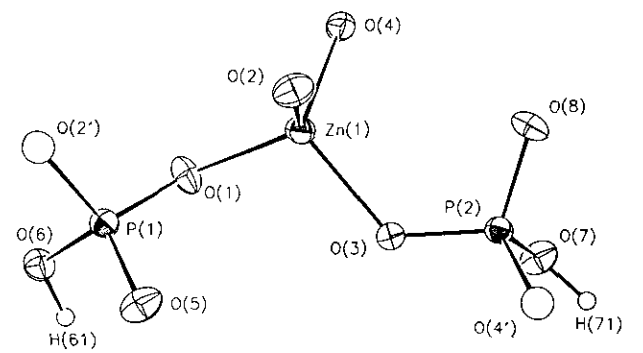

FIG. 1. ORTEP (22) view of the asymmetric Zn/P/O framework unit of $Na_2Zn(HPO_4)_2 \cdot 4H_2O$ showing the labeling scheme and 50% thermal ellipsoids (arbitrary-radius spheres for protons).

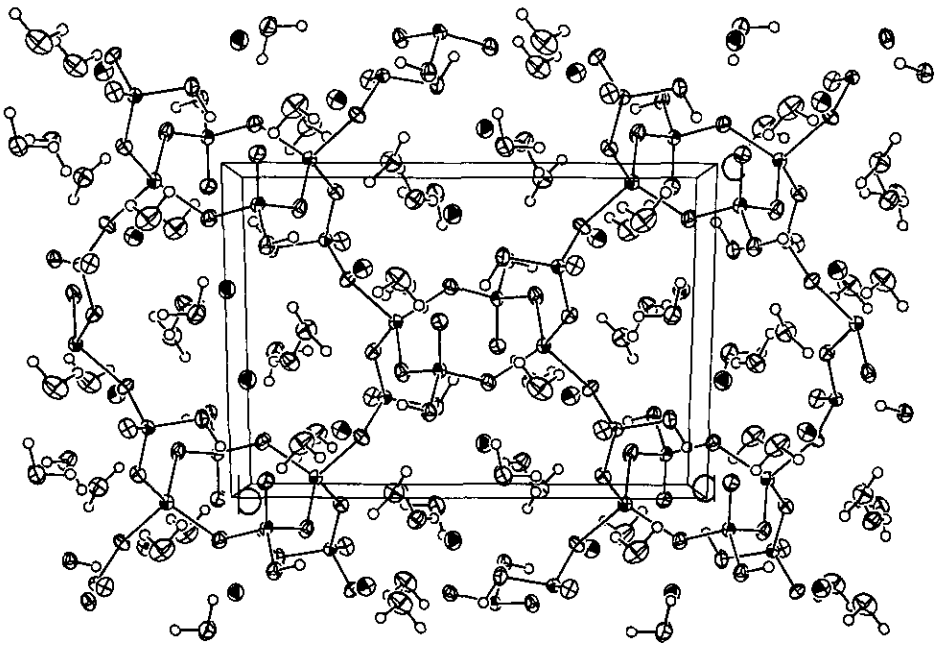

FIG. 2. ORTEP view down [100] of the $Na_2Zn(HPO_4)_2 \cdot 4H_2O$ crystal structure showing the pseudo-channels occupied by guest sodium cations (shaded ellipses) and water molecules (oxygen atoms, "open" ellipses).

in average bond lengths: d_{av}(P=O) = 1.517(3) Å; d_{av}(P–O_{Zn}) = 1.525(2) Å; and d_{av}(P–OH) = 1.575(3) Å. Similarly differentiated P=O, P–O_{Zn}, and P–OH bond lengths have been observed in other M/Zn/P/O materials such as the complex organo zincophosphates $Zn_4(PO_4)_2(HPO_4)_2 \cdot 3H_2O \cdot H_2N_2C_6H_{12}$ (9) and $Zn_5(PO_4)_2(HPO_4)_4 \cdot H_2O \cdot 2H_2N_2C_6H_{12}$ (10), and the layered $CsZn(PO_4)(HPO_4)$ and $NaZn(PO_4)(HPO_4)$ (12). Of the 12 crystallographically distinct oxygen atoms, four [O(1) to O(4)] make Zn–O–P bridges, with θ_{av} = 127.2°. Four more [O(5) to O(8)] are associated with P atoms [O(6) and O(7) are protonated], and the remaining four [O(10) to O(13)] are parts of "extra layer" water molecules.

The two crystallographically distinct sodium cations are both approximately octahedrally coordinated by oxygen atoms, with d_{av}[Na(1)–O] = 2.394(2) Å and d_{av} [Na(2)–O] = 2.472(2) Å. Na(1) has four water molecule oxygen atoms in its coordination sphere, and Na(2) has three H_2O neighbors. All the protons located in this X-ray study participate in H bonds, as indicated in Table 4. Only one intersheet H-bond connection exists as O(6)–H(61) ··· O(8): this is part of a P–OH ··· O=P link. The other P–OH group participates in an intrasheet

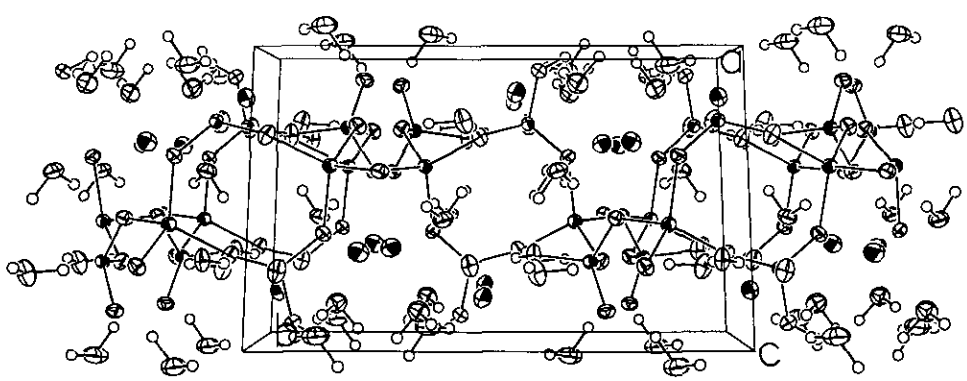

FIG. 3. ORTEP view down [001] of the $Na_2Zn(HPO_4)_2 \cdot 4H_2O$ crystal structure showing the infinite-layer structure and intra- and interlayer Na^+ cations and water molecules.

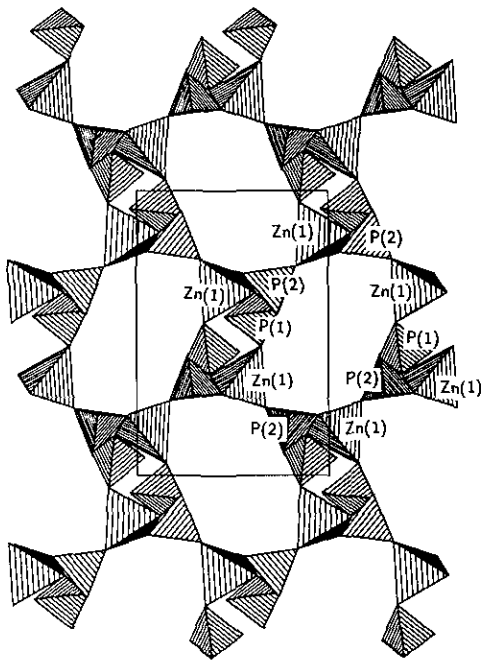

FIG. 4. STRUPLO (23) view down [100] of the Zn/P/O tetrahedral connectivity in $Na_2Zn(HPO_4)_2 \cdot 4H_2O$ showing the 12-ring topology, with one ring labeled to show the central-atom types involved.

P–OH · · · O=P link, perhaps offering additional stability to the open, 12-ring structure. The other H bonds are also intrasheet and involve a water-molecule proton to framework-oxygen linkage.

The connectivity of polyhedral units leads to the most significant structural feature of $Na_2Zn(HPO_4)_2 \cdot 4H_2O$ (Fig. 4)—a one-dimensional sheet structure of split, or "bifurcated," 12-rings, built up from 4-ring Zn(1)/P(1) tetrahedral subunits, linked via "bridging" P(2) groups. This [100] projection of the crystal structure of $Na_2Zn(HPO_4)_2 \cdot 4H_2O$ shows the presence of infinte, one-dimensional 12-ring "channels." These channels are not "continuous" as are those found in zeolite molecular sieves, but arise from alignment of the Zn/P/O/OH layers. Zn/P tetrahedral-atom alternation is therefore maintained by the bonding scheme in $Na_2Zn(HPO_4)_2 \cdot 4H_2O$: there are no Zn–O–Zn or P–O–P links in the structure. The Zn/P/O/H sheet, of formula $Zn(HPO_4)_2$, is anionic and is charge-balanced by the two sodium cations. Na(1) (Fig. 5) is roughly in the interlayer region, similar to the situation found in the layered material $NaH(ZnPO_4)_2$ (12), while Na(2) (Fig. 6) is more closely associated with one particular Zn/P/O/H sheet.

The ^{31}P MAS NMR spectra reported here are consistent with those expected on the basis of the crystallographic results for $Na_2Zn(HPO_4)_2 \cdot 4H_2O$. The $^{31}P\{^1H\}$ MAS NMR spectrum for $Na_2Zn(HPO_4)_2 \cdot 4H_2O$ (Fig. 7) confirms that the framework has two distinct phosphorus sites. The observed resonances fall well inside the range (~ −10 to +30 ppm) previously observed for a wide range of phosphate, pyrophosphate, and higher-polyphosphate-containing materials (19). In favorable cases (10, 19), an atom-to-peak assignment may be made based on the empirical relationship between up/downfield ^{31}P isotropic chemical shift and the sum of bond-valence sums (BVS) (20) of the oxygen atoms attached to the P atom in question. In this case, a value of Σ(BVS)[O(1), O(2), O(5), O(6)] = 7.24 for the four oxygen atoms surrounding P(1) results, including all H bonds (Table 4). A comparable value of Σ(BVS)[O(3), O(4), O(7), O(8)] for the P(2) nearest neighbors is 7.26. These Σ(BVS) values are indistinguishable for $Na_2Zn(HPO_4)_2 \cdot 4H_2O$, and the + 5.67- and +4.42-ppm peaks cannot be unambigously assigned to P(1) or P(2) in the structure.

CONCLUSIONS

The new structure of $Na_2Zn(HPO_4)_2 \cdot 4H_2O$ further expands the range of structure types in the Na/Zn/P/O phase space. The layered configuration of $Na_2Zn(HPO_4)_2 \cdot 4H_2O$ is somewhat similar to the puckered Zn/P/O/H layers found in $NaH(ZnPO_4)_2$ (12). However, the open 12-rings found in the layers are unprecedented in the hydrated-Zn/P/O system; the in-layer connectivity in $NaH(ZnPO_4)_2$ involves a more "condensed" arrangement in the layers, which includes tetrahedral 3-ring links (12).

As was found in our previous studies, it is relatively

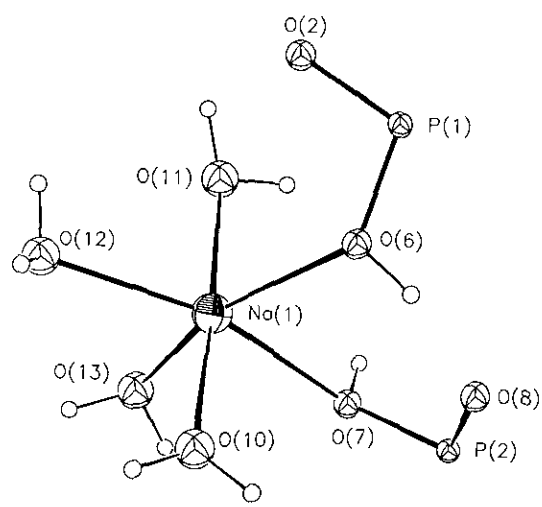

FIG. 5. ORTEP view of the Na(1) coordination polyhedron in $Na_2Zn(HPO_4)_2 \cdot 4H_2O$, with nearby "framework" bonds also indicated: 50% thermal ellipses; spheres of arbitrary radius for protons.

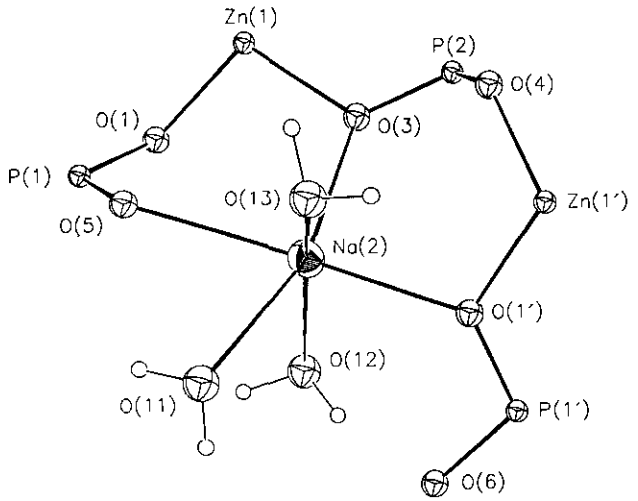

FIG. 6. ORTEP view of the Na(2) coordination polyhedron in $Na_2Zn(HPO_4)_2 \cdot 4H_2O$, with nearby framework bonds also indicated: 50% thermal ellipses; spheres of arbitrary radius for protons.

easy to form large (>0.5 mm) crystals of $Na_2Zn(HPO_4)_2 \cdot 4H_2O$ under mild conditions, suitable for characterization by standard single-crystal structure studies. This crystallization phenomenon is probably accounted for by the greater solubility of the zincophosphates and their precursors in these aqueous systems as compared to aluminosilicates and aluminophosphates, and the consequent opportunity for optimization of mild-condition kinetics in the synthesis procedure (13).

The variety of XO_4 (X = Zn, P) building blocks of these Zn/P/O tetrahedral structures (ZnO_4, ZnO_3OH_2, PO_4, PO_3OH, PO_3O_u, where O_u is an "unsaturated" P=O bond, PO_2O_uOH) allow the building-up of "interrupted," anionic tetrahedral networks, where some of the Zn–O–P links are replaced by the groups noted here. These may be particularly significant in establishing two-dimensional layer Zn/P/O-based structures, although it is not yet clear just which factors, kinetic or thermodynamic, direct a particular synthesis toward a one-dimensional (11), two-dimensional (12), or three-dimensional (10) structure. In the Zn/P/O systems, the protonated groups of the ZnO_3OH_2 and PO_3OH tetrahedra are structurally important and are usually involved in H bonds, as well as helping to offset the relatively high negative charge of the Zn/P/O network. Interrupted tetrahedral networks are much less common in framework aluminosilicate structures (21).

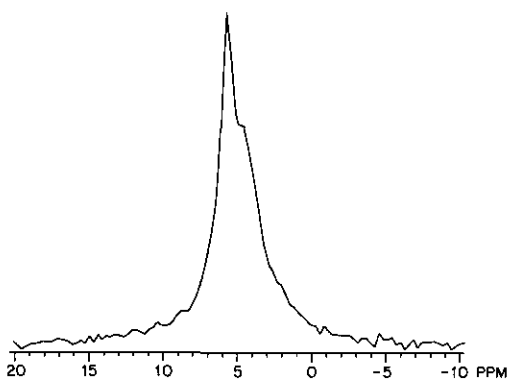

FIG. 7. $^{31}P\{^1H\}$ MAS NMR spectrum of $Na_2Zn(HPO_4)_2 \cdot 4H_2O$.

^{31}P MAS NMR spectral data for these phases are consistent with the crystallographic data, and may be qualitatively understood in terms of the relationship between phosphorus-atom chemical environment and its chemical shift (20). However, the rather consistent chemical environments of the phosphorus atoms in these materials do not always allow for an unambiguous peak-to-atom assignment.

Our synthetic studies of the hydrated-Na/Zn/P/O system are continuing: a novel family of zincophosphate phases, exemplified by $Na_3Zn_4O(PO_4)_3 \cdot 4H_2O$, based on an "all-tetrahedral" $ZnO_4/PO_4/OZn_4$ pharmacosiderite-like framework, are presently being characterized, and will be reported later.

ACKNOWLEDGMENT

We thank the National Science Foundation (Division of Materials Research) for partial financial support.

REFERENCES

1. P. B. Moore and J. Shen, *Nature (London)* **306,** 356 (1983).
2. M. Estermann, L. B. McCusker, Ch. Baerlocher A. Merrouche, and H. Kessler, *Nature (London)* **352,** 320 (1991).
3. V. Soghomonian, Q. Chen, R. C. Haushalter, J. Zubieta, and C. J. O'Connor, *Science* **259,** 1596 (1993).
4. T. E. Gier and G. D. Stucky, *Nature (London)* **349,** 508 (1991).
5. W. T. A. Harrison, T. E. Gier, K. L. Moran, J. M. Nicol, H. Eckert, and G. D. Stucky, *Chem. Mater.* **3,** 27 (1991).
6. T. M. Nenoff, W. T. A. Harrison, T. E. Gier, and G. D. Stucky, *J. Am. Chem. Soc.* **113,** 378 (1991).
7. T. E. Gier, W. T. A. Harrison, and G. D. Stucky, *Angew. Chem. Int. Ed. Engl.* **30,** 1169 (1991).
8. W. T. A. Harrison, T. E. Gier, and G. D. Stucky, *J. Mater. Chem.* **1,** 153 (1991).
9. W. T. A. Harrison, T. E. Martin, T. E. Gier, and G. D. Stucky, *J. Mater. Chem.* **2,** 175 (1992).
10. W. T. A. Harrison, T. M. Nenoff, M. M. Eddy, T. E. Martin, and G. D. Stucky, *J. Mater. Chem.* **2,** 1127 (1992).
11. W. T. A. Harrison, T. M. Nenoff, T. E. Gier, and G. D. Stucky, *Inorg. Chem.* **32,** 2437 (1993).
12. T. M. Nenoff, W. T. A. Harrison, T. E. Gier, J. C. Calabrese, and G. D. Stucky, *J. Solid State Chem.* **107,** 285 (1993).
13. T. E. Gier, W. T. A. Harrison, T. M. Nenoff, and G. D. Stucky, *in* "Synthesis of Microporous Materials, Volume 1: Molecular Sieves," p. 407. Van Nostrand–Reinhold, New York, 1992.
14. M. S. Lehmann and F. K. Larsen, *Acta Crystallogr. Sect. A* **30,** 580 (1974).
15. G. M. Sheldrick, "SHELXS-86 User Guide." Crystallography Department, University of Göttingen, Gemany, 1986.

16. D. J. Watkin, J. R. Carruthers, and P. W. Betteridge, "CRYSTALS User Guide." Chemical Crystallography Laboratory, Oxford University, UK, 1985.
17. A. C. Larsen, *in* "Crystallography Computing" (F. R. Ahmed, Ed.). Munksgaard, Copenhagen, 1970.
18. "International Tables for X-Ray Crystallography," Vol. IV. Kynock, Birmingham, 1974.
19. A. K. Cheetham, N. J. Clayden, C. M. Dobson, and R. J. B. Jakeman, *J. Chem. Soc. Chem. Commun.*, 195 (1986).
20. I. D. Brown and K. K. Wu, *Acta Crystallogr. Sect. B* **32,** 1957 (1976).
21. H.-R. Wenk, Z. *Kristallogr.* **137,** 113 (1973).
22. C. K. Johnson, Oak Ridge National Laboratory Report ORNL-5138, with local modifications. Oak Ridge, TN, 1976.
23. R. X. Fischer, *J. Appl. Crystallogr.* **18,** 258 (1985).